

2013-06-28

Influences of the Cinnamic Acid on Zinc Electrodeposition at Glassy-Carbon Electrode

Kai LI

Shen CHEN

Shen-na LIU

Bi-sang CHEN

Heng LIN

Guo-liang CHEN

Qing-xiang WANG

Recommended Citation

Kai LI, Shen CHEN, Shen-na LIU, Bi-sang CHEN, Heng LIN, Guo-liang CHEN, Qing-xiang WANG. Influences of the Cinnamic Acid on Zinc Electrodeposition at Glassy-Carbon Electrode[J]. *Journal of Electrochemistry*, 2013 , 19(3): Article 12.

DOI: 10.61558/2993-074X.2959

Available at: <https://jelectrochem.xmu.edu.cn/journal/vol19/iss3/12>

This Article is brought to you for free and open access by Journal of Electrochemistry. It has been accepted for inclusion in Journal of Electrochemistry by an authorized editor of Journal of Electrochemistry.

玻碳电极肉桂酸添加剂对锌电沉积的影响

李 凯, 陈 琴, 刘深娜, 陈碧桑, 林 珩, 陈国良*, 汪庆祥

(漳州师范学院化学与环境科学系, 福建 漳州 363000)

摘要: 用循环伏安法、计时电位法研究了玻碳电极肉桂酸添加剂对锌电沉积机理及成核过程的影响. 研究表明, 含肉桂酸基础镀液中还原仍为 $Zn^{2+} + 2e \rightarrow Zn$, 但肉桂酸能促进锌成核, 改变锌沉积的动力学过程. 在基础镀液锌成核机理为 3D-瞬时成核过程, 加肉桂酸后锌的成核机理趋于 3D-连续成核过程, 其活性位点数增加, 成核速率减小.

关键词: 锌电沉积; 肉桂酸; 成核及核生长; 计时电流法

中图分类号: O646

文献标识码: A

镀锌在钢铁防腐上有广泛的应用^[1-4]. Raecissi 等^[5]报道, 温度、pH 值及电流密度对锌沉积的成核机理、形态与结构有显著的影响. Yu 等^[6]发现, 温度升高成核密度增加, 并改变锌电沉积的成核机理. 此外, 锌离子浓度^[7]、阴离子^[8-9]、基质^[10]及添加剂^[11-13]等对锌沉积的过程均有较大影响, 而添加剂对锌沉积的形态结构及核生长机理影响最为明显. 少量添加剂 ($10^{-2} \sim 10^{-4} \text{ mol} \cdot \text{L}^{-1}$) 就可以获得结构致密、光亮度较好、耐腐蚀性强的锌镀层. 通常添加剂能吸附在电极表面, 影响活化能与电荷转移速率, 甚至改变电沉积机理^[14]. 吸附的添加剂分子部分覆盖于电极表面, 减少金属成核的活性位点数, 降低成核速率^[15-16]. Lee 等^[17]研究苯甲酸(BA)与聚乙烯醇(PEG)对锌沉积初始过程的影响, BA 与锌离子间有微弱的相互作用, 主要可控制锌镀层的粗糙度, 而 PEG 则吸附在电极表面, 提高锌及氢的还原过电位. Mackinnon 等^[18]报道, 在几种四烷基氯化铵中, 四丁基氯化铵的光亮镀层、细化晶粒与减小枝晶生长效果最好. Alvarez 等^[19]研究了硫酸盐镀锌过程中凝胶对锌在高定向热解石(HOPG)上电沉积的影响, 由于凝胶在 HOPG 表面成膜, 可使成核机理从瞬时成核变为连续成核. Trejo 等^[20]发现玻碳电极上聚乙烯醇能抑制锌的沉积, 改变锌初始阶段的成核过程, 且与聚乙烯醇的分子量有

关. Khosand 等^[21]发现, 尽管草酸根离子没有改变锌的成核机理, 但在草酸根离子的影响下, 锌在铁电极上成核数减少. Ballesteros 等^[22]报道无聚乙烯醇 20000, 锌的成核过程机理为 3D 扩散控制; 含有聚乙烯醇 20000, 锌的成核过程由两个同时进行的成核及生长过程组成, 即受 2Di-li 限制的 2D 瞬时成核过程与扩散控制的 3D 成核机理 (3D-dc). 此外, 硫脲、苄叉丙酮^[23]、山梨醇^[24]、香草醛^[25]和 1-丁基-3-甲基咪唑硫酸氢盐^[26]也是改善锌电沉积性能的常用添加剂.

尽管如此, 添加剂对锌沉积机理以及成核过程的影响仍然不甚清楚. 肉桂酸分子中含亚苄基, 有利于吸附在基质表面, 作为镀锌添加剂可增加镀层柔韧性, 是一种潜在的镀锌添加剂. 此外, 玻碳电极是一种惰性基质, 对氢有较高的过电位, 将其用于金属成核及核生长过程研究可忽略金属-金属间的相互作用^[20,27]. 本文用循环伏安法和计时电流法研究了玻碳电极在酸性硫酸盐溶液中锌电沉积过程及添加剂肉桂酸对锌电沉积机理的影响.

1 实验

1.1 试剂与仪器

高纯氮气, 七水合硫酸锌, 无水硫酸钠, 硼酸, 肉桂酸. 试剂均为分析纯, 溶液均由 Milli-Q 超纯水 ($18.2 \text{ M}\Omega \cdot \text{cm}$) 配制, 室温下测试.

收稿日期: 2012-04-18, 修订日期: 2012-05-24 * 通讯作者, Tel: (86-596) 2591445, E-mail: chengl259@126.com

国家自然科学基金项目(No. 20805041)、福建省科技厅高校产学研重大项目(No. 2010H6029)、福建省教育厅科技项目(No. JA10208)及漳州师范学院研究生教育创新基地资金项目资助

使用 PARC-263A 型恒电位仪 (Seiko EG&G), 通过 GPIB 接口卡 (EG & G) 和 M270 软件与计算机相连接, 完成数采集及分析. 玻碳工作电极 (GC, 面积 0.07 cm^2)、饱和甘汞参比电极 (SCE)、铂片辅助电极 ($1 \text{ cm} \times 1 \text{ cm}$) 和电镀溶液组成三电极体系.

1.2 玻碳电极处理

实验通 N_2 15 min 除氧. 玻碳电极分别用 $1 \mu\text{m}$ 、 $0.3 \mu\text{m}$ 以及 $0.05 \mu\text{m}$ 的氧化铝粉打磨, 50% 的乙醇溶液及纯水超声 5 min, 再用超纯水冲洗, 最后在铁氰化钾溶液 (含 $0.1 \text{ mol} \cdot \text{L}^{-1} \text{ KCl}$ 的 $1 \text{ mmol} \cdot \text{L}^{-1} \text{ Fe}(\text{CN})_6^{3-/4-}$) 中扫描, 扫描范围为 $-0.2 \sim 0.6 \text{ V}$, 获得重合的 CV 曲线即可^[20].

1.3 基础镀液组成

基础镀液 (S_0): $0.1 \text{ mol} \cdot \text{L}^{-1} \text{ ZnSO}_4 + 0.5 \text{ mol} \cdot \text{L}^{-1} \text{ Na}_2\text{SO}_4 + 0.08 \text{ mol} \cdot \text{L}^{-1} \text{ H}_3\text{BO}_3$, pH 4.39.

含肉桂酸基础镀液 (S_1): 基础镀液 (S_0) + $1 \text{ mmol} \cdot \text{L}^{-1}$ 肉桂酸, pH 4.39.

2 结果与讨论

2.1 循环伏安测量

1) 循环伏安曲线

图 1 给出了玻碳电极在基础镀液 (S_0) 及含肉桂酸基础镀液 (S_1) 中的循环伏安曲线, 扫描范围 $-0.20 \sim -1.60 \text{ V}$, 扫描速率 $50 \text{ mV} \cdot \text{s}^{-1}$. 从图 1 中可以看出, 在溶液 S_0 中, 负向电位扫描, -1.20 V 阴极电流开始增加, -1.38 V 出现阴极电流峰, 此为 Zn^{2+} 的还原 ($\text{Zn}^{2+} + 2\text{e} \rightarrow \text{Zn}$)^[20]. -1.60 V 正向电位扫描时, 此过程分别在阴极电流区与零电流区发生 2 次电流

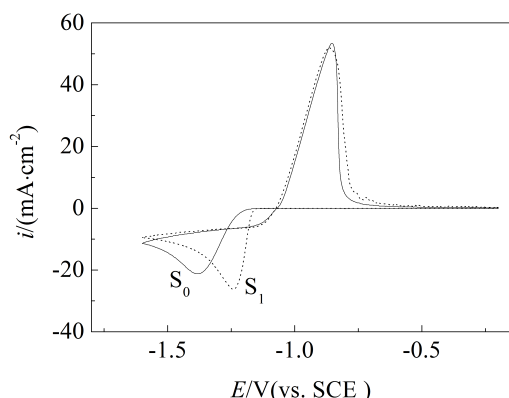


图 1 玻碳电极在基础镀液 (S_0) 与含肉桂酸基础镀液 (S_1) 中的循环伏安曲线 扫描速率: $50 \text{ mV} \cdot \text{s}^{-1}$

Fig. 1 Cyclic voltammograms of glassy carbon electrode in solutions with (S_1) and without (S_0) cinnamic acid Sweep rate: $50 \text{ mV} \cdot \text{s}^{-1}$

交叉, 表明电极表面有稳定的核生长中心形成^[28]. 阴极区电流交叉电位为 -1.26 V , 通常视为成核过电位 (Nucleation Overpotential, E_n)^[29]. 零电流区电流交叉电位是 -1.08 V (Crossover Potential, E_{CO}). 理论上 E_{CO} 等于沉积金属的标准还原电位 ($E_{CO} = E_{M^{n+}/M}$), 然而, 实验值比由 Nernst 方程计算值 (-1.04 V , $E_{\text{Zn}^{2+}} = -1.01 - 0.03 \text{ pZn}^{2+}$) 更负, 这是因为锌在 GC 电极沉积存在着过电位. 继而正向电位扫描, 在 -0.85 V 处出现一个阳极峰, 该峰应为锌氧化.

含肉桂酸的基础镀液, 其循环伏安曲线仍然存在两次电流交叉, 且 E_{CO} 不变, 表明肉桂酸并没有影响锌的沉积机理. 肉桂酸使 E_n 明显正移 (-1.18 V), 影响锌沉积的动力学过程. 此外, 其还原峰电位 (-1.24 V , E_{cp}) 正移, 峰电流增大, 说明肉桂酸促进锌的沉积. Mo 等^[30] 研究苯甲酸钠对氯化钾溶液中锌沉积过程影响, 当苯甲酸钠浓度为 $0.007 \text{ mol} \cdot \text{L}^{-1}$ 时能促进锌的沉积. 低浓度的苯甲酸钠削弱电极/溶液间的作用力促进锌成核. 显然, 肉桂酸与苯甲酸钠的作用相似.

表 1 给出了两种镀液锌氧化及还原电量参数. 含肉桂酸的基础镀液 (S_1) 中, Q_a 及 Q_c 值均增大, Q_a/Q_c 比值亦递增, 说明肉桂酸能促进锌的沉积.

表 1 在基础镀液 (S_0) 与含肉桂酸基础镀液 (S_1) 中锌氧化还原电量参数

Tab. 1 Charge parameters of zinc oxide reduction in solutions with (S_1) and without (S_0) cinnamic acid

Solution	$ Q_c / (\text{mC} \cdot \text{cm}^{-2})$	$Q_a / (\text{mC} \cdot \text{cm}^{-2})$	$Q_a / Q_c $
S_0	185.85	147.20	0.79
S_1	201.27	180.04	0.90

2) 扫描速率

图 2 为玻碳电极在 S_0 与 S_1 溶液阴极峰电流 $-i_{cp}$ 随扫描速率平方根 $v^{1/2}$ 变化的关系曲线. 两种溶液中 $-i_{cp}$ 与 $v^{1/2}$ 均呈线性, 说明锌的还原过程均受扩散控制; 拟合直线截距大于 0 点, 说明伴有其它的动力学过程发生, 该过程可能涉及成核过程^[31]. 含肉桂酸基础镀液 (S_1) 的拟合直线截距更大, 成核过程更加明显, 肉桂酸削弱了电极/溶液之间的作用力, 有更多的活性位点促进锌的沉积.

3) 不同转换电位

图 3 和图 4 给出了基础镀液 (S_0) 和含肉桂酸

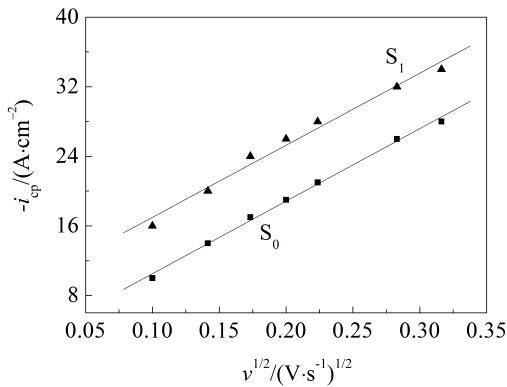


图2 玻碳电极在基础镀液(S₀)与含肉桂酸基础镀液(S₁)中的*-i_{cp}* - *v*^{1/2}曲线

Fig. 2 Variation of the peak current density (*-i_{cp}*) with the square root of sweep potential rate (*v*^{1/2}) for zinc deposition on glassy carbon electrode in solutions with (S₀) and without (S₁) cinnamic acid

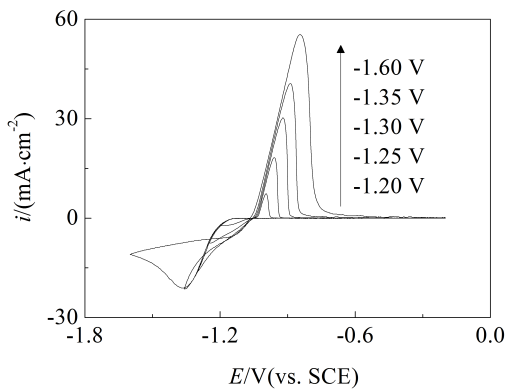


图3 玻碳电极在基础镀液(S₀)中不同转换电位*E_λ*的循环伏安曲线

Fig. 3 Cyclic voltammograms showing the effect of switching potential (*E_λ*) on zinc deposition in S₀ solution on glassy carbon electrode

基础镀液(S₁)中不同转换电位*E_λ*下的循环伏安曲线. 由图3可知,不同转换电位下,*E_{CO}*均保持不变. 随*E_λ*值正移,其阳极峰电流减小,峰电位负移. S₁溶液中(图4),*E_{CO}*也不随*E_λ*而变化,随*E_λ*值正移,其阳极峰电流减小且出现一小的肩峰,归因于肉桂酸作用下形成了含添加剂分子的锌沉积相^[30].

2.2 锌成核机理计时电流分析测量

图5和图6为玻碳电极在基础镀液(S₀)和肉桂酸在基础镀液(S₁)中锌电沉积初始电位阶跃电流-时间暂态曲线. 由图5可知,不同阶跃电位下其

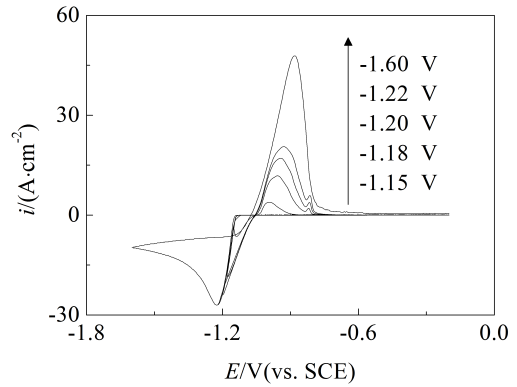


图4 玻碳电极在含肉桂酸基础镀液(S₁)中不同转换电位*E_λ*的循环伏安曲线

Fig. 4 Cyclic voltammograms showing the effect of switching potential (*E_λ*) on zinc deposition in S₁ solution on glassy carbon electrode

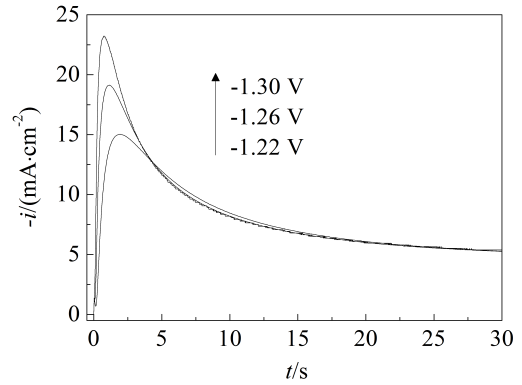


图5 玻碳电极在基础镀液(S₀)中不同阶跃电位锌电沉积*i-t*暂态曲线

Fig. 5 Chronoamperometric curves for the zinc electrocrystallisation on glassy carbon electrode in S₀ solution

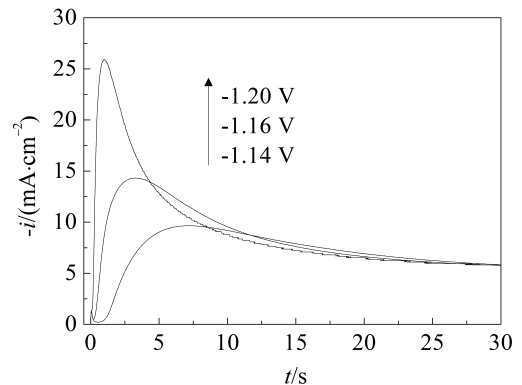


图6 玻碳电极在含肉桂酸基础镀液(S₁)不同阶跃电位锌*i-t*暂态曲线

Fig. 6 Chronoamperometric curves for the zinc electrocrystallisation on glassy carbon electrode in S₁ solution

$i-t$ 曲线相似,短时间内电流增大达到最大值,而后电流减小,趋向于某一稳定值.这是典型的3D成核过程^[32-33]. $t < t_m$ 时,双电层充电,同时金属离子放电,晶核形成和生长使电流上升, t_m 时刻达到极大值 i_m ,此时Zn的电结晶过程经历了生长中心的交叠.之后瞬态电流逐渐衰减并趋向于稳定值,表明锌离子稳定扩散至电极表面^[34].

瞬时成核过程:成核数比较大,电极的活性位点瞬间被晶核覆盖.3D瞬时成核电流 i 与时间的关系如式(1):

$$\left(\frac{i}{i_m}\right)^2 = 1.5942 \left(\frac{t}{t_m}\right)^{-1} \left\{ 1 - \exp \left[-1.2564 \left(\frac{t}{t_m}\right) \right] \right\}^2 \quad (1)$$

连续成核过程:成核数依赖于时间.电流与时间的关系如式(2):

$$\left(\frac{i}{i_m}\right)^2 = 1.2254 \left(\frac{t}{t_m}\right)^{-1} \left\{ 1 - \exp \left[-2.3367 \left(\frac{t}{t_m}\right)^2 \right] \right\}^2 \quad (2)$$

式中, i_m 最大电流密度, t_m 对应 i_m 的时间.

由式(1)、(2)拟合可得到3D成核的 $(i/i_m)^2$ 对 t/t_m 无因次理论曲线,将实验值 $(i/i_m)^2$ 对 t/t_m 作无因次曲线,与理论曲线比较就可分析成核过程.

图7给出了图5相对应不同电位玻碳电极在基础镀液锌沉积无因次实验值与理论值曲线.显然,锌成核机理趋向3D-瞬时成核,该过程受扩散控制. Alvarez等^[35-37]研究酸性硫酸盐锌沉积也得出类似结果.

含肉桂酸基础镀液在不同的阶跃电位下, $i-t$ 曲线相似,电流先增大, t_m 时刻达到最大值 i_m ,随

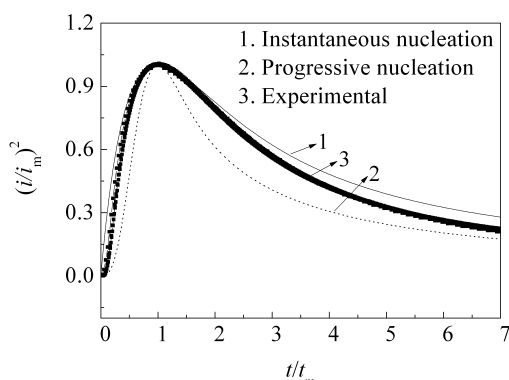


图7 玻碳电极在基础镀液(S_0)不同阶跃电位锌电沉积的无因次 $(i/i_m)^2-t/t_m$ 曲线

Fig. 7 Dimensionless $(i/i_m)^2$ vs. (t/t_m) plots for zinc electrodeposition on glassy carbon electrode in S_0 solution at different potentials

后减小,并趋向极限值,说明肉桂酸存在时锌的成核过程为3D-成核过程.图8给出了与图6相对应不同电位玻碳电极含肉桂酸基础镀液(S_1)无因次实验值与理论值曲线.溶液中存在肉桂酸时,其锌成核机理更接近连续成核过程.值得注意的是, S_0 和 S_1 溶液中,无因次电流时间曲线的 t/t_m 值大于1时,实验结果逐渐偏离理论曲线,说明电结晶过程中沉积于玻碳电极表面上的锌可能逐渐引发析氢过程.

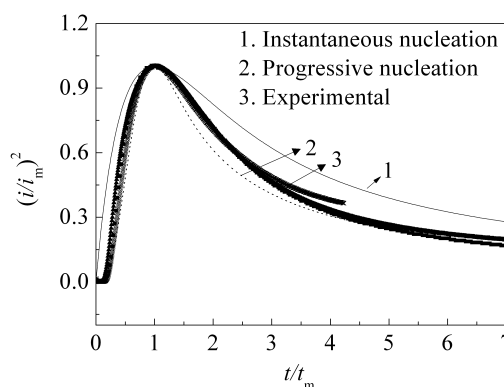


图8 玻碳电极在含肉桂酸基础镀液(S_1)不同阶跃电位锌电沉积的无因次 $(i/i_m)^2-t/t_m$ 曲线

Fig. 8 Dimensionless $(i/i_m)^2$ vs. (t/t_m) plots for zinc electrodeposition on glassy carbon electrode in S_1 solution at different potentials

Scharifker与Hull理论已广泛用于讨论成核过程中的瞬间成核模式与过程成核模式,但用该理论不能准确获得动力学参数.在此基础上,Scharifker与Mostany提出新理论^[38],该理论可获得动力学参数而不需要区别成核过程.通过该理论给出3D扩散控制理论方程(式(3))对单步暂态曲线进行非线性拟合,就可得扩散系数 D 、活性位点数 N_0 及成核速率常数 A 等动力学参数.

$$i(t) = \left(\frac{zFD^{1/2}c}{\pi^{1/2}t^{1/2}} \right) \left\{ 1 - \exp \left[-N_0 \pi k^* D \left(t - \frac{(1-e^{-At})}{A} \right) \right] \right\} \quad (3)$$

式中, $k^* = (8\pi cM/\rho)^{1/2}$, i 为电流密度($A \cdot cm^{-2}$), F 为法拉第常数($C \cdot mol^{-1}$), z 为电荷数, D 为扩散系数($cm^2 \cdot s^{-1}$), c 为摩尔浓度($mol \cdot cm^{-3}$), M 为锌的相对原子质量($g \cdot mol^{-1}$), ρ 为沉积金属的密度($g \cdot cm^{-3}$), N_0 为活性位点数或最大晶核数密度(cm^{-2}), A 为成核速率常数(s^{-1}).表2、表3分别列出不同阴极电

位下瞬态电流-时间曲线的动力学参数. 从表看出, 随着阴极电位的负移, 成核速率常数 A 及活性位点数均增大, 说明两种镀液中的成核机理均为扩散控制的 3D 成核过程.

图 9 给出玻碳电极在基础镀液(S_0)和含肉桂酸基础镀液(S_1)分别在 -1.30 V 与 -1.16 V 电位阶跃下锌电沉积实验与式(3)非线性拟合的理论 $i-t$ 曲

线. 其实验值与拟合曲线非常吻合, 其它阶跃电位下其拟合曲线的 R^2 也均大于 0.98 (见表 2、3), 说明实验获得的电流密度归因于扩散控制的 3D 成核及生长. 在 S_0 溶液中, 其成核速率常数 A 较大, 活性位点数 N_0 较小, 还原过程初级阶段表面趋于饱和, 随后发生瞬时成核过程, 低 N_0 值与高 A 值导致成核半径增大(因此沉积金属的粒径大). 在 S_1

表 2 玻碳电极在基础镀液(S_0)不同阶跃电位的瞬态电流动力学参数

Tab. 2 Kinetic parameters extracted from the current transients on GC from S_0 solution

E/V	$D/(10^{-6}\text{ cm}^2\cdot\text{s}^{-1})$	$N_0/(10^{-6}\text{ cm}^2)$	A/s^{-1}	t_m/s	$i_m/(\text{mA}\cdot\text{cm}^{-2})$	R^2
-1.34	5.90	1.16	10.58	0.51	27.63	0.9961
-1.30	5.64	0.88	7.80	0.76	23.21	0.9960
-1.26	5.66	0.61	4.70	1.12	19.12	0.9960
-1.22	5.92	0.35	2.61	1.95	15.02	0.9952
-1.20	6.28	0.26	1.97	2.48	13.79	0.9943
-1.18	6.47	0.16	1.32	3.73	11.24	0.9920

表 3 玻碳电极在含肉桂酸基础镀液(S_1)不同阶跃电位的瞬态电流动力学参数

Tab. 3 Kinetic parameters extracted from the current transients on GC from solution containing cinnamic acid (S_1)

E/V	$D/(10^{-6}\text{ cm}^2\cdot\text{s}^{-1})$	$N_0/(10^{-6}\text{ cm}^2)$	A/s^{-1}	t_m/s	$i_m/(\text{mA}\cdot\text{cm}^{-2})$	R^2
-1.20	6.86	2.59	0.71	1.00	25.85	0.9919
-1.19	6.66	1.71	0.53	1.41	21.10	0.9916
-1.18	6.85	0.63	1.09	1.77	18.58	0.9925
-1.16	7.39	0.26	0.92	3.22	14.31	0.9935
-1.15	7.39	0.15	0.88	4.48	11.93	0.9957
-1.14	7.64	0.16	0.18	7.08	9.63	0.9853

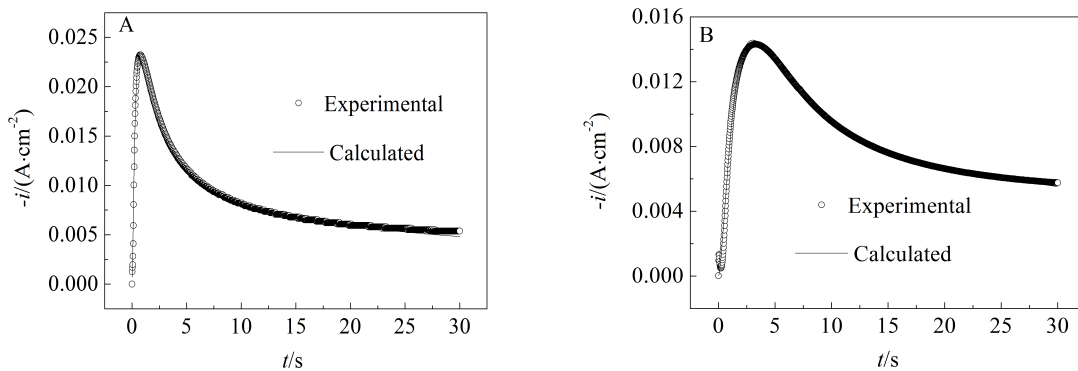


图 9 玻碳电极在基础镀液(S_0 , A)和含肉桂酸基础镀液(S_1 , B)阶跃电位分别为 $E = -1.30\text{ V}$ 与 $E = -1.16\text{ V}$ 锌电沉积实验瞬态与理论瞬态 $i-t$ 曲线

Fig. 9 Comparison of an experimental transient recorded at $E = -1.30\text{ V}$ in S_0 (A) and $E = -1.16\text{ V}$ in S_1 (B) with a typical transient on GC

溶液中,成核速率常数 A 减小,活性位点数 N_0 增大,发生连续成核过程,此过程中肉桂酸的吸附阻碍了活性位点的增加,有利于缩小沉积物粒径。

3 结 论

酸性硫酸盐基础镀液锌的还原过程为 $Zn(II) \rightarrow Zn(0)$,肉桂酸并没有改变其反应机理。肉桂酸减小锌的沉积过电位,增加阴极峰电流密度,对锌的电沉积起促进作用。

基础镀液锌成核机理为扩散控制的 3D-瞬时成核过程,含肉桂酸基础镀液,锌成核机理趋于扩散控制的 3D-连续成核过程,其活性位点数 N_0 增大,成核速率 A 减小,利于晶粒细化。

参考文献(References):

- [1] Barcelo G, Sarret M, Muller C, et al. Corrosion resistance and mechanical properties of zinc electrocoatings[J]. *Electrochimica Acta*, 1998, 43(1): 13-20.
- [2] Rajendran S, Bharanti S, Krishna C. Electrodeposition of zinc-cobalt alloy from cyanide-free alkaline plating bath [J]. *Plating and Surface Finishing*, 1997, 84(10): 53-57.
- [3] Hosny A Y, Rofei M E, Ramadan T A, et al. Corrosion resistance of zinc coatings produced from a sulfate bath[J]. *Metal Finishing*, 1995, 93(11): 55-59.
- [4] Bozzini B, Accardi V, Cavallotti P L, et al. Electrodeposition and plastic behavior of low-manganese zinc-manganese alloy coatings for automotive applications[J]. *Metal Finishing*, 1999, 97(5): 33-33.
- [5] Raeissi K, Saatchi A, Golozar M A. Effect of nucleation mode on the morphology and texture of electrodeposited zinc[J]. *Journal of Applied Electrochemistry*, 2003, 33(7): 635-642.
- [6] Yu J, Wang L, Su L, Ai X, et al. Temperature effects on the electrodeposition of zinc[J]. *Journal of The Electrochemical Society*, 2003, 150(1): C19-C23.
- [7] Trejo G, Ortega B R, Meas Y, et al. Nucleation and growth of zinc from chloride concentrated solutions[J]. *Journal of The Electrochemical Society*, 1998, 145(12): 4090-4097.
- [8] Sanchez Cruz M, Alonso F, Palacios J M. Nucleation and growth of zinc electrodeposits on a polycrystalline zinc electrode in the presence of chloride ions[J]. *Journal of Applied Electrochemistry*, 1993, 23(4): 364-370.
- [9] Yu J, Yang H, Ai X, et al. Effects of anions on the zinc electrodeposition onto glassy-carbon electrode[J]. *Russian Journal of Electrochemistry*, 2002, 38(3):363-367.
- [10] Aleksandar R D, Miomir G P. Deposition of zinc on foreign substrates[J]. *Electrochimica Acta*, 1982, 27(11): 1539-1549.
- [11] Song K D, Kim K B, Han S H, et al. Effect of Additives on hydrogen evolution and absorption during Zn electrodeposition investigated by EQCM[J]. *Electrochemical and Solid-State Letters*, 2004, 7(2): C20-C24.
- [12] Mockute D, Bernotiene G. Behaviour of benzylidene acetone during zinc electrodeposition in weakly acid solution containing a nonionic surfactant and/or carboxylic acid [J]. *Journal of Applied Electrochemistry*, 1997, 27 (6): 691-694.
- [13] Yu J, Chen Y, Yang H, Huang Q. The influences of organic additives on zinc electrocrystallization from KCl solutions[J]. *Journal of The Electrochemical Society*, 1999, 146(5): 1789-1793.
- [14] Michailova E, Peykova M, Stoychev D, et al. On the role of surface active agents in the nucleation step of metal electrodeposition on a foreign substrate [J]. *Journal of Electroanalytical Chemistry*, 1994, 366(1/2): 195-202.
- [15] Simanavicius L, Stakenas A, Sarkis A. The initial stages of aluminum and zinc electrodeposition from an aluminum electrolyte containing quaternary aralkylammonium compound [J]. *Electrochimica Acta*, 1997, 42(10): 1581-1586.
- [16] Michailova E, Vitanova I, Stoychev D, et al. Initial stages of copper electrodeposition in the presence of organic additives[J]. *Electrochimica Acta*, 1993, 38(16): 2455-2458.
- [17] Lee J Y, Kim J W, Lee M K, et al. Effects of organic additives on initial stages of zinc electroplating on iron[J]. *Journal of The Electrochemical Society*, 2004, 151 (1): C25-C31.
- [18] Mackinnon D J, Brannen J M. Evaluation of organic additives as levelling agents for zinc electrowinning from chloride electrolytes[J]. *Journal of Applied Electrochemistry*, 1982, 12(1): 21-31.
- [19] Alvarez A E, Salinas D R. Nucleation and growth of Zn on HOPG in the presence of gelatine as additive[J]. *Journal of Electroanalytical Chemistry*, 2004, 566(2), 393-400.
- [20] Trejo G, Ruiz H, Ortega B R, et al. Influence of polyethoxylated additives on zinc electrodeposition from acidic solutions[J]. *Journal of Applied Electrochemistry*, 2001, 31(6): 685-692.
- [21] Khorsand S, Raeissi K, Golozar M A. Effect of oxalate anions on zinc electrodeposition from an acidic sulphate

- bath[J]. *Journal of The Electrochemical Society*, 2011, 158 (6): D377-D383.
- [22] Ballesteros J C, Díaz-Arista P, Meas Y, et al. Zinc electrodeposition in the presence of polyethylene glycol 20000 [J]. *Electrochimica Acta*, 2007, 52 (11): 3686-3696.
- [23] Li M C, Jiang L L, Zhang W Q, et al. Electrodeposition of nanocrystalline zinc from acidic sulfate solutions containing thiourea and benzalacetone as additives[J]. *Journal of Solid State Electrochemistry*, 2007, 11(4): 549-553.
- [24] Oliveira E M, Carlos I A. Voltammetric and morphological characterization of zinc electrodeposition from acid electrolytes containing boric-polyalcohol complexes[J]. *Journal of Applied Electrochemistry*, 2008, 38(9): 1203-1210.
- [25] Kim S J, Kim H T, Parka S M. Effects of o-vanillin as a brightener on zinc electrodeposition at iron electrodes[J]. *Journal of the Electrochemical Society*, 2004, 151 (12): C850-C854.
- [26] Zhang Q, Hua Y. Effects of 1-butyl-3-methylimidazolium hydrogen sulfate-[BMIM]HSO₄ on zinc electrodeposition from acidic sulfate electrolyte [J]. *Journal of Applied Electrochemistry*, 2009, 39(12): 261-267.
- [27] Luis H, Clara H, María G. Zinc electrodeposition from chloride solutions onto glassy carbon electrode[J]. *Journal of the Mexican Chemical Society*, 2009, 53(4): 243-247.
- [28] Gomes A, Da-Silva-Pereira M I. Zn electrodeposition in the presence of surfactants Part I. Voltammetric and structural studies[J]. *Electrochimica Acta*, 2006, 52 (3): 863-871.
- [29] Fletcher S. Some new formulae applicable to electrochemical nucleation/growth/ collision [J]. *Electrochimica Acta*, 1983, 28(7): 917-923.
- [30] Mo Y, Huang Q, Li W, et al. Effect of sodium benzoate on zinc electrodeposition in chloride solution[J]. *Journal of Applied Electrochemistry*, 2011, 41(7): 859-865.
- [31] Morón L E, Meas Y, Ortega B R, et al. Effect of a poly(ethylene glycol) (MW 200)/benzylideneacetone additive mixture on Zn electrodeposition in an acid chloride bath [J]. *International Journal of Electrochemical Science*, 2009, 4(12): 1735-1753.
- [32] Gunawardena G, Hills G, Montenegro I, et al. Electrochemical nucleation: Part I. General considerations[J]. *Journal of Electroanalytical Chemistry*, 1982, 138 (2): 225-239.
- [33] Gunawardena G, Hills G, Montenegro I. Electrochemical nucleation: Part V. Electrodeposition of cadmium onto vitreous carbon and tin oxide electrodes[J]. *Journal of Electroanalytical Chemistry*, 1985, 184(2): 371-389.
- [34] Abyaneh M Y. Modelling diffusion controlled electrocrystallisation processes[J]. *Journal of Electroanalytical Chemistry*, 2006, 586(2): 196-203.
- [35] Alvarez A E, Salinas D R. Nucleation and growth of Zn on HOPG in the presence of gelatine as additive[J]. *Journal of Electroanalytical Chemistry*, 2004, 566(2): 393-400.
- [36] Despic A R, Pavlovic G. Deposition of zinc on foreign substrates[J]. *Electrochimica Acta*, 1982, 27(11): 1539-1549.
- [37] Breen J M, Gannon E. Electrodeposition of zinc on glassy carbon from ZnCl₂ and ZnBr₂ electrolytes[J]. *Journal of The Electrochemical Society*, 1983, 130(8): 1667-1670.
- [38] Scharifker B R, Mostany J. Three-dimensional nucleation with diffusion controlled growth: Part I. Number density of active sites and nucleation rates per site[J]. *Journal of Electroanalytical Chemistry*, 1984, 177(1/2): 13-23.

Influences of the Cinnamic Acid on Zinc Electrodeposition at Glassy-Carbon Electrode

LI Kai, CHEN Shen, LIU Shen-na, CHEN Bi-sang, LIN Heng,

CHEN Guo-liang*, WANG Qing-xiang

*(Department of Chemistry and Environment Science, Zhangzhou Normal University,
Zhangzhou 363000, Fujian, China)*

Abstract: The influences of cinnamic acid (CIN) on the mechanism of Zn deposition and nucleation kinetics onto glassy-carbon electrode were studied by cyclic voltammetry (CV) and chronoamperometry (CA). The results revealed that the zinc reduction took place via $\text{Zn}^{2+} + 2\text{e} \rightarrow \text{Zn}$ in the presence of CIN, but the kinetics of zinc deposition was changed and the formation rate of zinc nuclei was accelerated. In the absence of CIN, the mechanism of zinc nucleation followed the 3D-instantaneous diffusion-controlled nucleation, while the 3D-progressive diffusion-controlled nucleation in the presence of CIN. The addition of CIN reduced the nucleation rate, but increased the number of active sites as compared with those obtained without CIN.

Key words: zinc electrodeposition; cinnamic acid; nucleation and growth; chronoamperometry